Spectral sensitivity transition in the compound eyes of a twilight-swarming mayfly and its visual ecological implications*

Ádám Egri[1,‡], Ádám Mészáros[1,2,3], György Kriska[1,3]

1: Institute of Aquatic Ecology, Centre for Ecological Research, H-1113 Budapest, Karolina út 29, Hungary

2: Doctoral School of Environmental Sciences, Eötvös University, H-1117 Budapest, Pázmány sétány 1, Hungary

3: Group for Methodology in Biology Teaching, Biological Institute, Eötvös University, H-1117 Budapest, Pázmány sétány 1, Hungary

‡ Corresponding author, e-mail address: egri.adam@ecolres.hu

Abstract

Aquatic insect species that leave the water after larval development, such as mayflies, have to deal with extremely different visual environments in their different life stages. Measuring the spectral sensitivity of the compound eyes of the virgin mayfly (*Ephoron virgo*) resulted in differences between the sensitivity of adults and larvae. Larvae were primarily green-, while adults were mostly UV-sensitive. The sensitivity of adults and larvae was the same in the UV, but in the green spectral range, adults were 3.3 times less sensitive than larvae. Transmittance spectrum measurements of larval skins covering the eye showed that the removal of exuvium during emergence cannot explain the spectral sensitivity change of the eyes. Taking numerous sky spectra from the literature, the ratio of UV and green photons in the skylight was shown to be maximal for $\theta \approx -13°$ solar elevation, which is in the θ_{min} = -14.7° and θ_{max} = -7.1° typical range of swarming that was established from webcam images of real swarmings. We suggest that spectral sensitivity of both the larval and adult eyes are adapted to the optical environment of the corresponding life stages.

Keywords: ERG, *Ephoron virgo*, visual ecology, insect vision, imago, larva

Introduction

Mayflies (Ephemeroptera) are winged aquatic insects originating from the Carboniferous period, with approximately 3300 currently known species [1]. They live primarily in freshwater systems on all continents except for Antarctica. Mayflies spend most of their life at the bottom of water bodies as larvae and they are very short-lived as adults. The adults do not feed, their only objective is reproduction. Emergence can happen continuously without a well defined swarming period, but a number of species, specifically the burrowing mayflies such as *Ephoron* (Polymitarcyidae) or *Palingenia* species (Palingeniidae) can emerge in enormous numbers on a single day during the swarming period [1].

The virgin mayfly [*Ephoron virgo* (Olivier, 1791)] is such a species being present in several rivers of Europe. This species gained attention in the past decades because during their mass swarming, millions of individuals are attracted to illuminated areas and bridges resulting in mass mortality [2–5]. The life cycle of *E. virgo* is one year. Eggs hatch into larvae in spring around April [6,7]. During the approximately

*The contents of this document was adjusted to exactly match the contents of the published paper: Egri Á, Mészáros Á, Kriska G. 2022 Spectral sensitivity transition in the compound eyes of a twilight-swarming mayfly and its visual ecological implications. Proc. R. Soc. B. 289, 20220318. (doi:10.1098/rspb.2022.0318)

four months of development (electronic supplementary material, movie S1), larvae live in the littoral zone down to a depth of 6 m [8] in the uppermost layer of the river bottom in U-shaped tubes, where they feed on suspended particles [9]. At the end of the summer the swarming period comes. After sunset, the larvae ascend to the surface, the adults emerge in the river current, and they immediately take off to minimize the risk of predation by fish [1]. During emergence the thorax and abdomen become inflated with air which facilitates the emergence itself [10]. Males need an additional moult for becoming mature imagos (electronic supplementary material, movie S2), while in the case of females the sub-imago is the reproductive stage [10]. After copulation above the river surface, when the natural illumination is almost completely dark for the human eye, the females start their compensatory flight upstream above the river (electronic supplementary material, movies S3 and S4) to compensate for the downstream drift of the population and finally lay their eggs into the river [11] (electronic supplementary material, movie S5). This is a typical behaviour of river-dwelling mayflies. The adults do not last longer than the night of the swarming [9]. The synchronized emergence of mayflies at twilight is a very impressive phenomenon (electronic supplementary material, movies S3 and S4), which might be driven by temperature and light intensity [1].

In a recent study, when our primary aim was to optimize a phototaxis-based mayfly protecting system [12] (electronic supplementary material, movie S4), we revealed that the attraction of *E. virgo* and another twilight-swarming mayfly (*Caenis macrura* Stephens, 1836) to light is the highest for UV and blue light and decreases with increasing wavelength [13]. Similar results were reported for other, non-identified twilight-swarming mayfly species [14]. On the other hand, it is a well-known phenomenon that the relative amount of short wavelength radiation (UV and blue) in the spectrum of the skylight is highest during twilight when the sun is below the horizon, but sunlight scattered in the atmosphere is still dominating the sky [15]. Parallelism between the previously mentioned spectral sensitivity of phototaxis of *E. virgo* and the UV- and blue-rich spectral characteristics of the sky during the time of swarming led us to measure the spectral sensitivity of compound eyes of *E. virgo* adults with electroretinography (ERG). Although remarkable changes in the anatomy of eyes throughout different life stages both for females and males have been shown in *Cloeon* sp. [16], spectral sensitivity of any mayfly eyes has been measured only in extremely few cases, and as far as we know, no larvae were measured. Hence, we also measured the spectral sensitivity of larvae. In this study, we demonstrate how the compound eyes of the virgin mayfly are optimized for the optical environment both in the larval and adult life stages.

Material and Methods

Mayflies

Larvae were collected from the river Ipoly near Letkés (Northern Hungary, 47° 53′ 08.2″ N 18° 45′ 48.0″ E) on several mornings between 3 June and 5 August 2020. Adults were collected at evenings after sunset between 6 and 16 August 2020 at the nearby bridge where a few public lights usually attract mayflies. Larvae and adults were transported to the laboratory in river-water-containing jars and plastic containers, respectively, inside a conventional cooler box. High humidity for the adults inside the plastic containers was ensured by wet kitchen papers. In the laboratory, the animals were kept at 10°C temperature. ERG recordings on larvae were performed within 36 h after collection, typically between 5:00 and 15:00 (UTC + 2 h). Recordings on adults were started at dawn around 5:00 (UTC + 2 h; 5-6 h after collection) and were continued until no alive specimens were available (typically around 11:00; 11-12 h after collection).

Electroretinography recordings

The preparation of adults and larvae was quite similar. The insects were laid on a 2 × 2 cm (thickness = 2 mm) transparent Plexiglas and a piece of adhesive tape was used to fix their body to the Plexiglas. The abdomen and thorax of larvae and adults were covered with the tape. In the case of larvae, a water droplet was inserted under the tape to ensure a wet surroundings for the gills on the abdomen and a second piece of adhesive tape was used to fix the mandibles to the Plexiglas. In the case of adults, the mandibles were fixed to the Plexiglas with a droplet of melted paraffin wax.

Microelectrodes composed of tungsten wire (diameter = 0.08 mm) etched in saturated KNO_2 solution were used for recordings. Measuring and reference electrodes were inserted into the right eye and between the head and thorax, respectively. Photoreceptor responses were amplified with a custom-built amplifier (see electronic supplementary material figure S1 in Kecskeméti et al. [17]). For data acquisition

we used a USB sound card based on the C-Media CM6206 USB Audio I/O Controller chip (C-Media Electronics Inc., Taipei, Taiwan), which was modified for low-frequency measurements based on the instructions available on the Data AcQuisition And Real-Time Analysis website (http://www.daqarta.com). Recordings were made with the free Audacity 2.2.1 audio recording software (https://www.audacityteam.org). Time course of the amplified photoreceptor responses was recorded by the left channel of the sound card, while the right channel was used for recording a reference signal indicating the presence of the light stimuli. The reference signal was used for calibrating the voltage level on the left channel and ensured the identification of the receptor responses in the recorded data (16-bit WAV format, sampling frequency = 8 kHz). In preliminary tests, the linearity of the sound card inputs was verified within the ±1V range, thus amplification was set to keep the measured signals far within this range.

Light stimuli were created with a LED-based, custom-built light source being able to create 14 different quasi-monochromatic light stimuli with a light intensity variable over several log intensity units (for more details see Egri & Kriska [18]). For creating light stimuli, we used the following 12 wavelengths (± half bandwidth of LED): 346 nm (± 5.0 nm), 376 nm (± 4.8 nm), 402 nm (± 5.5 nm), 421 nm (± 6.4 nm), 442 nm (± 8.5 nm), 467 nm (± 10.4 nm), 496 nm (± 13.5 nm), 516 nm (± 14.5 nm), 552 nm (± 17.7 nm), 598 nm (± 6.9 nm), 623 nm (± 7.7 nm), 641 nm (± 8.6 nm).

After a 30 min of dark adaptation, a preprogrammed stimulus sequence was presented to the eye preparation. The distance of the eye from the light guide was the same for all measurements (d = 2.5 mm). For a given wavelength, 7-8 500-ms-long stimuli with logarithmically increasing intensities (intensity step ≈ 0.5 log unit) were presented to the preparation with 6-s-long dark inter-stimulus intervals. This scan was performed for all 12 wavelengths in increasing and reversed wavelength order with 12-s-long dark periods when switching wavelength. The whole sequence was repeated 2-4 times. Photon flux of light stimuli varied between 2.5×10^{10} and 7.6×10^{14} photons cm^{-2} s^{-1}.

The magnitude of negative jumps in potential during the first 100 ms of a light stimulus was considered as the response amplitude. In the case of a given stimulus sequence, for each wavelength, response amplitudes were plotted against log photon flux of light stimuli and sigmoid exposure-response functions were fitted on the data. Reciprocals of photon fluxes required for eliciting a standard response criterion (0.1 mV) were calculated for all wavelengths and the spectral sensitivities obtained for each stimulus sequence repetition were averaged. Out of the total number of 73 collected larvae and approximately 2500 collected adults, spectral sensitivity of 19 larval (14 females + 5 males) and 14 adult (13 females + 1 male) compound eyes were successfully measured with ERG.

The above-mentioned measurement protocol allowed us to compare the sensitivity curve of larvae and adults on the same plot. For each of the preparation groups of female larvae, female adults and male larvae, the differences in absolute sensitivity of the individuals were removed with the method described by Allan et al. [19]. In short, all spectral sensitivity curves within a group were normalized with their integral, which resulted in curves fitting on each other. Finally, all curves were scaled with the same constant in such a way that the mean sensitivity at 516 nm became the same value as the mean of the original sensitivities at 516 nm. This method turned out to be robust, because using the other wavelengths for scaling produced practically the same final spectral sensitivity curves. The sensitivity curve of the single male adult was not adjusted.

Since the measured spectral sensitivities were bimodal, the sum of two A1-based pigment templates (equations (1)-(5) in [20]) was fitted to the mean spectral sensitivity of female and male larvae and female adults. Since each template had two free parameters (λ_{max} and a vertically scaling parameter), the sum of two templates had four parameters. The fit was performed with the downhill simplex method [21]. No curve was fitted to the spectral sensitivity of the single measured male.

Transmittance spectrum of exuviae

Since we found differences between larval and adult spectral sensitivities, the question arose whether these differences can be explained by the lack of exuvium after the final moult of the larva. The transmittance spectrum of *E. virgo* exuviae at the cornea lens was measured with an Ocean Optics STS-VIS spectrometer equipped with a P400-010-UV-VIS fibre (Ocean Optics, Largo, USA). Exuviae of *E. virgo* were collected from the surface of the river Ipoly when *E. virgo* were emerging in huge numbers, and were kept in 10°C river water until the next morning. From each exuvium, a region (diameter = 1.5-2 mm) containing one of the array of cornea lenses were manually cut out under a stereo microscope and were inserted into a thin layer of water between two coverslips. The area of the cornea lens array was

approximately 20% of the separated section of the exuvium. Measurements were performed outdoors, the fibre terminal (core diameter = 400 μm) was directed to the clear blue sky which was used as a light source. The sample sandwiched between the coverslips was inserted in front of the fibre terminal and a spectrum was measured. Another spectrum was taken with slightly biased position of the sample so that the measured light propagated through only the two coverslip layers and the encompassed thin water layer. Dividing the former spectrum with the latter resulted in the transmittance spectrum. A total number of 6 (3 females + 3 males) transmittance spectra were measured, each for separate exuviae.

Because cornea lens arrays of *E. virgo* exuviae were very small and were not easy to handle, as a reference, we measured the transmittance spectrum of cornea lenses of a *Libellula depressa* Linnaeus, 1758 dragonfly exuvium with the same method. Measurement on the bigger array of cornea lenses (diameter = 2-3 mm) could be reliably performed.

Swarming period of *E. virgo* within the day

The intensity of *E. virgo* swarming as a function of solar elevation was determined from images of a public webcam directed to a lamp-lit Danube embankment section in Budapest (Hungary, 47° 28′ 46.6″ N 19° 03′ 32.7″ E). Daily webcam time-lapse videos were downloaded from http://camvid.idokep.hu/thuthu and were selected for further evaluation if swarming *E. virgo* mayflies were apparent around the urban lights. Archived images of this webcam was a potentially useful information source of mayfly swarmings between 2012 and 2021. Videos from seven, seven and four evenings proved to be usable in 2012, 2014 and 2019, respectively. In Budapest, *E. virgo* is the only insect species being able to perform such intense swarming that could be seen on these webcam images, thus *E. virgo* was not confused with other species.

After extracting the frames from a given day's time-lapse video (8-bit JPG) (electronic supplementary material, figure S1A, B), for each frame the corresponding solar elevation θ was calculated from the time and location and a conspicuous lamp and its intimate vicinity was cropped from the frames (electronic supplementary material, figure S1C). Further evaluation involved only frames taken after sunset ($\theta < 0°$). The median of the cropped sub-images was calculated (electronic supplementary material, figure S1D), it was subtracted from all original sub-images and finally the resultant sub-images were converted to greyscale (electronic supplementary material, figure S1E). This resulted in a series of processed images where bright pixels on a black background represented the swarming mayflies (electronic supplementary material, figure S1E). For each processed image, the overall image brightness obtained by calculating the mean of pixel intensities was considered as a measure of swarming intensity. Thus, for each evaluated day, a curve was established quantifying the swarming intensity as a function of solar elevation. For all evaluated days of 2012, 2013 and 2019, these curves were averaged resulting in yearly mean curves, and the median was subtracted from each yearly curve to move the baseline to zero. The full widths at 25% maximum of the peak in each mean curve were considered as the typical solar elevation range of the swarming for each year: $[\theta_{min}, \theta_{max}]_{2012}$, $[\theta_{min}, \theta_{max}]_{2013}$ and $[\theta_{min}, \theta_{max}]_{2019}$. Finally the union of these yearly ranges was considered as the quantified typical solar elevation range of swarming of *E. virgo* mayflies. It is important to mention that this method detected the beginning of the swarming (emergence with copulation and upstream compensatory flight) with a time delay, because the mayflies must have already started their flight before arriving to the urban lights observed by the webcam.

Optical environment of larvae and adults

Besides measuring the spectral sensitivity of the compound eyes of *E. virgo* adults and larvae, we were also interested in the spectral characteristics of different optical environments that are being observed by these mayflies in their different life stages. First we made an attempt to get an insight into the visual world of the larvae. At the same place where larvae were collected for ERG recordings, a radiometrically calibrated and cosine corrector-equipped (CC-3-UV-S) Ocean Optics STS-VIS spectrometer (Ocean Optics, Largo, USA) was used to measure and compare the spectrum of the underwater and terrestrial world. Here, the river flows towards South. From the Eastern shore, around noon on 2 July 2020 (typically 4 weeks before swarming, solar elevation = 48.3°, solar azimuth = 111.4°, a partly cloudy day), two spectra were measured with horizontal orientation of the cosine corrector towards the Western shore of the approximately 20-m-wide river (figure 1A). One measurement was made 50 cm above the water level, and another underwater at a depth of 20 cm. In the latter case, the spectrometer was placed into an aquarium that was submerged in the water. The transmittance spectrum of the aquarium wall was taken into account. These spectra were measured only for demonstration purposes and were just plotted.

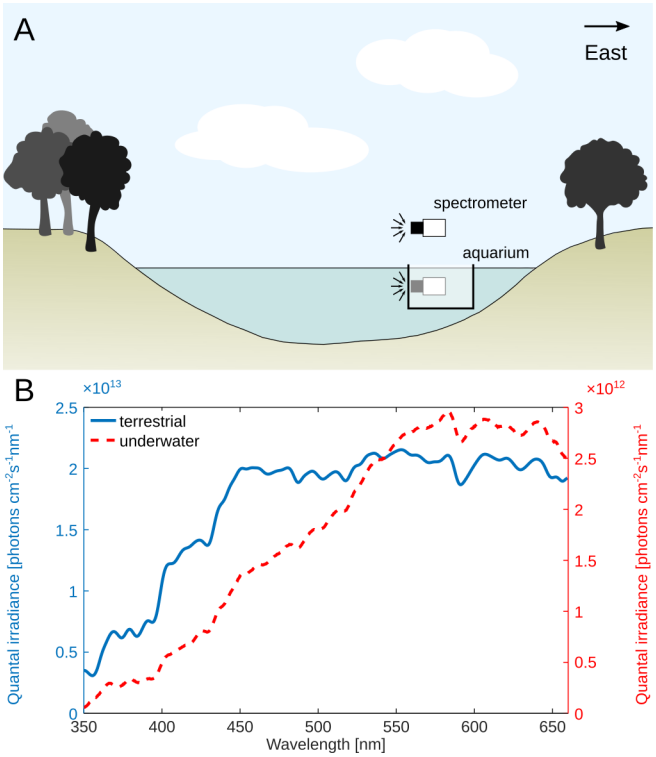

Figure 1: Measured spectra of the terrestrial and underwater environment at the location where *E. virgo* larvae were collected. (A) Schematic diagram of the scene where the two spectral measurements were made. (B) Measured spectra above (blue solid line) and under (red dashed line) the water level.

Bearing in mind the bimodal spectral sensitivity of adults, we performed a simple analysis on the UV/green content of various skylight spectra as a function of solar elevation. Skylight spectra were used from the supplementary material of Spitschan et al. [22], who have measured hundreds of clear sky spectra in a rural environment under various solar elevations and moon phases at the latitude of 41° 39′ 52.6″ N during the summer of 2014. We used spectra that were measured in the -23° < θ < 23° solar elevation range. First, these sky spectra originally given in energy units were converted to quantal irradiance units (photons cm^{-2} s^{-1} nm^{-1}) as described by Johnsen [23]. Taking into account the fitted sensitivity maxima of the adult UV and green receptors, for each sky spectrum corresponding to a given solar elevation, the integral of irradiances in the 365 nm ± 5 nm and 516 nm ± 5 nm ranges, and their ratio was calculated (for most sky spectra the lowest available wavelength was 360 nm).

We made an attempt to measure sky spectra with our previously mentioned spectrometer, but for solar elevations below -5° the measured spectra lost in noise as noted by Johnsen [23]. Therefore, using spectra from the literature was far more effective.

Statistics

Spectral sensitivity of female larvae and adults was compared wavelength by wavelength with Mann-Whitney U tests, as well as the spectral sensitivity of male and female larvae. Tests were performed with the statistics package of GNU Octave 5.2.0.

Results

Spectral sensitivity of the compound eyes of *E. virgo* larvae and adults

Typical measured receptor responses of a female *E. virgo* larva and an adult for different stimulus intensities are shown in electronic supplementary material, figure S2. The grey regions represent the 500-ms-long light stimuli and the stimulus intensities are also displayed in optical density units defined as OD = $-\log_{10}(I/I_0)$, where $I_0 = 7.59 \cdot 10^{14}$ photons cm^{-2} s^{-1}.

Mean spectral sensitivity of female larvae and adults with the fitted sum of pigment templates are shown in electronic supplementary material, figure 2 with vertical bars denoting s.d. Blue and red curves correspond to larvae and adults, respectively. Both curves are bimodal having sensitivity maxima in the UV and green spectral range. Larvae are mostly sensitive to the green, while the sensitivity of adults is the highest for the UV range. It is also clear that in the UV range (λ < 400 nm) the sensitivity of larvae and adults are practically the same, while for longer wavelengths, the adult eyes are significantly less sensitive than the eyes of larvae. At 516 nm, the adult eye is approximately 3.3 times less sensitive than the larval eye. For each tested wavelength, asterisks at the bottom of the figure indicate statistically significant differences between the larvae and adults emerged from Mann-Whitney U tests at $\alpha = 0.001$ significance level. Solid curves indicate the fitted sum of pigment templates, while the dotted and dashed curves are, respectively, the templates corresponding to the assumed UV and green receptor types. Maxima of the fitted templates for the female larvae are λ_{max}^{UV} = 373 nm, and λ_{max}^{G} = 530 nm. For the female adults λ_{max}^{UV} = 364 nm, and λ_{max}^{G} = 516 nm were obtained. In the case of both UV and green receptor types, the peak wavelength was shifted towards the shorter wavelengths. Because of these emerged differences between the corresponding peak wavelengths of larvae and adults, we performed the same curve fitting separately for each preparation. This enabled us to statistically compare the peak wavelengths of larvae and adults with Mann-Whitney U tests. The mean of these separate wavelengths for the assumed UV and green pigments for female larvae and adults were the same as the previously mentioned λ_{max}^{UV} and λ_{max}^{G} values within the difference range of $\pm$ 1 nm. According to the Mann-Whitney U tests, the peak wavelength of UV sensitivity of the larvae and adults was practically similar (p = 0.047, z = -1.990), while the shift in peak wavelength of the assumed green receptor was significant (p < 0.01, z = -2.669).

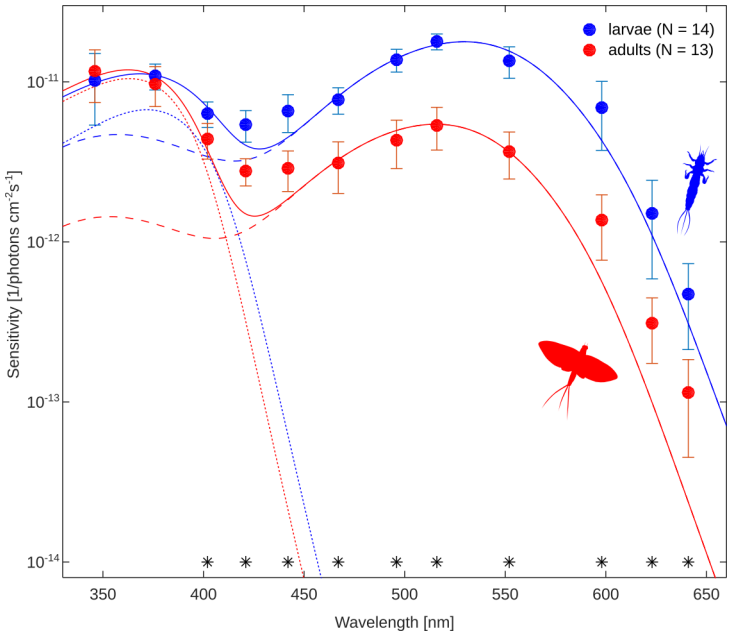

Figure 2: Mean spectral sensitivity of the compound eye of female *E. virgo* larvae and adults. Vertical bars denote s.d. and asterisks at the bottom indicate significant differences between sensitivity of larvae and adults revealed by Mann-Whitney U tests ($\alpha = 0.001$). Blue and red continuous curves show the fitted sum of two A1-based pigment templates for the larvae and adults, respectively. The two corresponding A1-based pigment templates (UV and green) are shown by dotted and dashed curves.

Figure 3 shows the spectral sensitivity of male larvae and the single male adult with the same concept as that of figure 2. The male larval spectral sensitivity is practically the same as we measured for the females (blue curves in figures 2, 3). This was verified with Mann-Whitney U tests, which detected a significant sensitivity difference between female and male larvae only at the single wavelength of 516 nm. Sensitivity maxima of the simultaneously fit two pigment templates for the male larvae are λ_{max}^{UV} = 379 nm, and λ_{max}^{G} = 522 nm. The spectral sensitivity of the single measured male adult is shown by the red curve. It is important to note that this cannot be reliably compared with the other curves because this is a single measurement. Receptor response amplitudes varied between preparations, and without having more preparations, the absolute sensitivities could not be averaged out (see Methods).

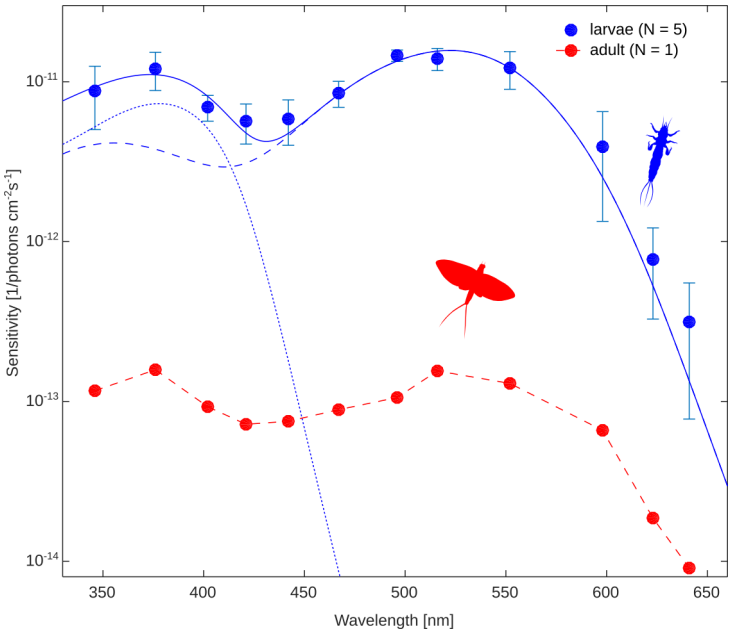

Figure 3: Spectral sensitivity of the compound eye of male *E. virgo* larvae and the single adult. Vertical bars denote s.d. for larvae. The blue continuous curve shows the fitted sum of two A1-based pigment templates for the larvae. The two corresponding A1-based pigment templates (UV and green) are shown by dotted and dashed curves. The spectral sensitivity of the single male adult is just plotted with linear interpolation between the datapoints.

Transmittance spectrum of exuviae

Figure 4 displays the mean transmittance spectrum of the six measured *E. virgo* exuviae and the transmittance of the single *L. depressa* exuvium. The two curves are qualitatively similar, the transmittance decreases with decreasing wavelength.

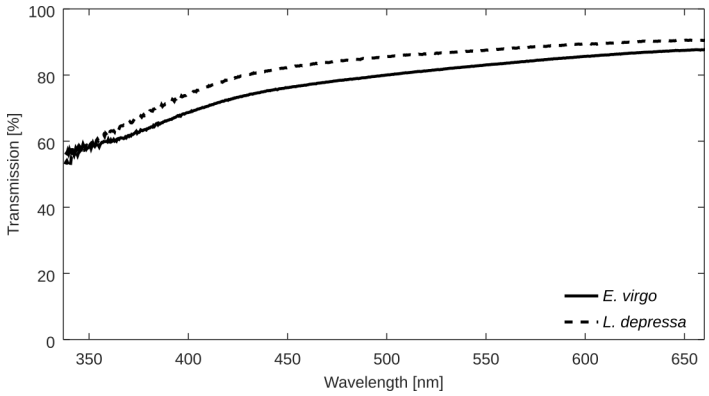

Figure 4: Transmittance spectrum of *E. virgo* and *L. depressa* exuviae. Solid line: mean transmittance spectrum of the six measured *E. virgo* exuviae. Dashed line: Transmittance spectrum of the *L. depressa* exuvium.

Swarming period of *E. virgo* within the day

Electronic supplementary material, figure S3 shows the yearly mean of quantified swarming intensities as a function of solar elevation for the years 2012 (electronic supplementary material, figure S3A), 2013 (electronic supplementary material, figure S3B) and 2019 (electronic supplementary material, figure S3C) obtained from the webcam time-lapse videos. Horizontal dotted lines show the 25% level of the maximal value in each graph. In the case of the years 2012, 2013 and 2019 typical solar elevation ranges of swarming (full width at 25% maximum) were $[\theta_{min}, \theta_{max}]_{2012}$ = [-13.7°, -7.7°], $[\theta_{min}, \theta_{max}]_{2013}$ = [-10.5°, -7.1°] and $[\theta_{min}, \theta_{max}]_{2019}$ = [-14.7°, -12°], respectively. These intervals are represented with yellow rectangles in the

graphs. The range of solar elevations within which mayflies swarmed in these 3 years is indicated by the red vertical dashed lines. Thus, according to our webcam-based method, *E. virgo* mayflies typically swarm between θ_{min} = -14.7° and θ_{max} = -7.1° solar elevations.

Optical environment of larvae and adults

Measurement of the spectral characteristics of the terrestrial and underwater environment at the collection site of the larvae resulted in the spectra shown in figure 1B. It is clear that the underwater visual environment is relatively poor in short wavelengths, which is not surprising because the river water usually has a brownish appearance for the human eye. On the other hand, the total photon flux under the water was approximately 10 times lower than above the water level (ratio of the areas below the curves in figure 1B equals 9.7). This means that UV and blue light are filtered out and longer wavelengths dominate the much dimmer underwater world at a typical site where *E. virgo* larvae develop.

Ratio of UV and green photons as a function of solar elevation is plotted in figure 5A. Each cross in figure 5 corresponds to UV/green ratio calculated from a skylight spectra obtained from Spitschan et al. [22]. The thick red line shows the moving average of the datapoints calculated with a 3-degree-wide window. The pair of dashed vertical lines represents the solar elevation range obtained from webcam images for the typical swarming period (electronic supplementary material, figure S1, Fig. S3). According to figure 5, the ratio of the number of UV (365 nm ± 5 nm) and green (516 nm ± 5 nm) photons in the natural skylight illumination is constant during the day (θ > 10°), starts to increase when sunset is approaching (0° < θ < 10°), peaks around θ ≈ −13° in the interval, when *E. virgo* mayflies really perform swarming (electronic supplementary material, figure S3), and finally decrease when starlight and/or moonlight start to dominate the sky (θ < -18°).

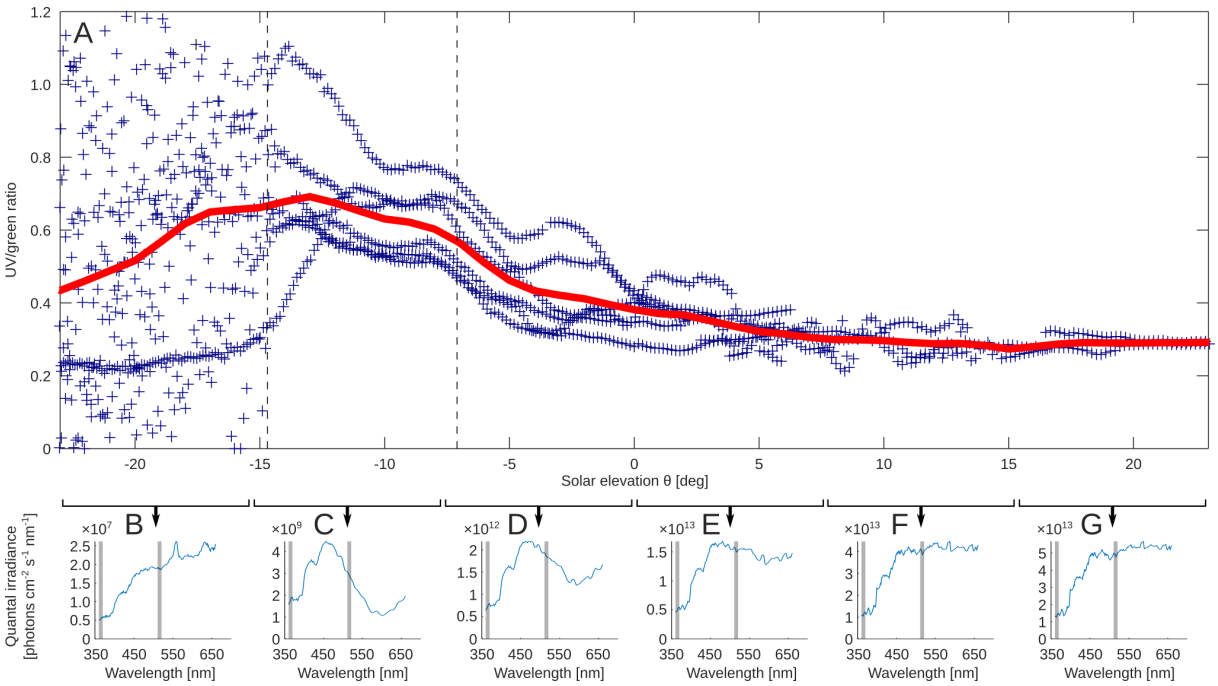

Figure 5: Spectral characteristics of the sky as a function of solar elevation. (A) Content ratio of UV (365 nm ± 5 nm) and green (516 nm ± 5 nm) photons in the spectrum of the sky as a function of solar elevation θ for various spectra measured by Spitschan et al. [22]. Thick red curve is the moving average calculated with a window width of 3 degrees. Typical solar elevation range of swarming of *E. virgo* (electronic supplementary material, figure S3) is indicated by a pair of vertical dashed lines. (B) Mean spectrum in the -23° < θ < -15.3° solar elevation range. For calculating the UV/green content ratio, the spectra were integrated in the 10-nm-wide windows shown by grey rectangles. (C) As B for -15.3° < θ < -7.7°. (D) As B for -7.7° < θ < 0°. (E) As B for 0° < θ < 7.7°. (F) As B for 7.7° < θ < 15.3°. (G) As B for 15.3° < θ < 23°.

Figure 5B-G shows the mean sky spectra corresponding to 7.7 degree-wide solar elevation ranges indicated by horizontal brackets under the horizontal axis of figure 5A. Thus each curve in figure 5B-G is the average of all sky spectra obtained from Spitschan et al. [22], that corresponded to the solar ele-

vaion range shown by the horizontal brackets. The purpose of figure 5B-G is to demonstrate the spectral changes in the sky spectrum in six steps in the -23° < θ < 23° solar elevation range. Each individual spectrum was used to calculate a UV/green ratio indicated by a blue cross in figure 5A. In figure 5B-G, grey rectangles show the wavelength ranges in which the integral of a given spectrum was calculated for the UV (365 nm ± 5 nm) and green (516 nm ± 5 nm) regions.

Discussion

Spectral sensitivity measurements of compound eyes of mayfly adults are very scarce in the literature, possibly because the short lifespan of the individuals. In our case, mortality was extremely high, only 14 *E. virgo* adult individuals could be measured out of the approximately 2500 collected individuals. Previous studies on certain *Ephemera* and *Atalophlebia* mayflies have shown that their compound eyes are maximally sensitive to UV light [24,25], which is in accordance with our results. The reader should have noticed that we measured the spectral sensitivity of only a single male adult. The reason for this lies in the swarming behaviour of *E. virgo* and our collection technique. We collected mayflies around urban lights where the individuals were attracted. They were practically all females, because the compensatory upstream flight is performed exclusively by females [5].

Regarding *E. virgo* larvae, our ERG recordings represent the first attempt to measure the spectral sensitivity of any mayfly larvae, as far as we know. We propose that the high green-sensitivity of the compound eyes of the larvae, relative to the UV-sensitivity is related to the spectral characteristics of the natural underwater environment of larvae. Larvae of several Ephemeroptera species seem to be negatively phototactic [26,27], and are more active in darkness [28]. However, there are mayfly species, the larvae of which are slightly attracted to long-wavelength (green-yellow) light [29]. According to our personal observations, *E. virgo* larvae are negatively phototactic which is not surprising from a burrowing mayfly that lives inside the upper layer of the river bottom. Our spectral measurements showed that the underwater environment in a typical river where *E. virgo* larvae develop is extremely long-wavelength-dominant, thus short wavelengths like UV are mostly lacking from the illumination. On the other hand, the light intensity was also remarkably lower inside the river water. As our measurements were performed at a depth of only 20 cm, the relative amount of short wavelength radiation is generally much lower at the river bottom, as well as the overall light intensity. According to Kühne et al. [29], phototaxis of aquatic insects living exclusively in water (e.g. larvae) is generally long-wavelength-sensitive.

However, the subjective measure of visual perception sensed by the insect may differ from the ERG-determined sensitivities; the spectral sensitivity of female adults shows a sensitivity decrease in the green spectral range relative to the sensitivity of larvae, but the UV-sensitivity remains at the same level. The underwater optical environment of the larvae is more long-wavelength-dominant and dimmer than that of the terrestrial environment in any conditions, because the differences depend on the reflection and transmission characteristics of the underwater objects and the river water, respectively. Emerging adults get into a brighter environment with higher content of short wavelength illumination, thus losing green sensitivity might not be disadvantageous. In addition, crepuscular and twilight-active insects tend to have relatively highly UV-sensitive eyes [25,30].

The difference between the spectral sensitivity of larvae and adults begs additional questions about the timing of the change in sensitivity. According to the measured transmittance spectrum of the larval skin, the removal of the exuvium should increase the sensitivity over the whole spectrum, and this increase itself should increase towards the short wavelengths. In relative terms, the larval eyes are approximately 1.6 times more sensitive in the green than in the UV region. In the case of adults, the eyes are approximately two times sensitive in the UV than in the green range. Thus, taking into account the transmittance spectrum of the larval skin, the final moult alone cannot account for the sensitivity of adults compared to the larvae. Consequently, the spectral sensitivity change must be mainly the result of changes in the eye itself. It is important to note that our corneal transmittance measurements were not the most precise, however our results were similar to that of Meyer-Rochow and Horridge [31], who measured the transmittance of a terrestrial beetle. Nevertheless, compared to other measurements of corneal transmission [32], our measured transmittance spectra are lower, thus it would be worth to perform measurements in a microspectrophotometer. We measured the ERG of larvae of various size including the final larval stage when the forewing pads become very dark just before the final moult [1]. We found that the sensitivity of larvae was quite uniform and we did not find any larvae having spectral sensitivity resembling the adults' sensitivity curve. Thus, the transition in sensitivity must happen relatively quickly around the

time of the final moult, because adults must have well prepared eyes for their few-hours-long life which is the final and most important element of their 1-year-long life cycle. Opsin expression changes during larval development of certain mayflies have already been identified [33,34], which might be the case for *E. virgo* also. To mention another resembling case, daily changes in gene expression of a long-wavelength opsin were reported in a firefly, while no change was detected in the UV-opsin expression [35]. Changes in opsin expression could decrease the concentration of photopigments in the green receptors of *E. virgo* adults. This could result in the decrease of sensitivity, because the sensitivity of a photoreceptor depends on the concentration of photopigments in the receptor [36]. On the other hand, the decrease in the number of green photoreceptors could also account for the lower green sensitivity of adults. Daily changes in eye spectral sensitivity is not uncommon among arthropods [36]. In our case, the recordings on larvae and adults were not exactly, but approximately performed in the same period of the day, thus the emerged differences between larval and adult sensitivities were not likely due to diurnal variation in spectral sensitivity.

In our analysis, we concluded that *E. virgo* typically swarms between -14.7° and -7.1° solar elevations (electronic supplementary material, figure Fig. S3), when the relative amount of UV photons compared to that of the green photons is maximal (figure 5). Taking into account that the swarming period of *E. virgo* typically takes place between the beginning of August to mid-September, the previously mentioned solar elevation range corresponds to an approximately 1-h-long interval. However, it is important to note that the swarming starts earlier than the time of θ = -7.1° because our webcam method detected the appearance of mayflies around urban lights and did not detect the emergence and copulation which can take place earlier, before the upstream compensatory flight of the females. From electronic supplementary material, figure S3, it seems that the beginning of the detected swarmings are not exactly the same for the studied years. The reason for this may lie in the compensatory flight. The time course of swarming intensity at a given location can vary during swarming because the time of the females' arrival depends on the spatial distribution of emergence downstream from the observed location. Each year, the spatial distribution of the oviposition events may vary due to the weather, light pollution, for example, which may determine the spatial distribution of emergence events of the next year. These yearly spatial fluctuations in emergence locations can result in different dynamics in swarming intensity at a given location.

Similar to many other aquatic insects, *E. virgo* adults possess positive polarotaxis to horizontally polarized light and have the ability to visually detect water surfaces by means of the water-reflected horizontally polarized light [37]. The polarization sensitivity of aquatic insects usually works in the UV or blue spectral range, because the degree of polarization of light reflected from natural water surfaces is highest for short wavelengths [38,39]. To mention two extreme examples, the degree of polarization of light reflected from a dark water surface can be more than 2.5 times higher in the UV than in the green, while for an eutrophic, green-brown-looking pond, the same ratio can be approximately 1.2, which is still greater than 1 [38]. This phenomenon is independent of solar elevation, which is the main determinant of light conditions [39]. In behavioural experiments Schwind [38] found that *Cloeon* sp. (Ephemeroptera: Baetidae) use the blue spectral region for detecting polarization of light. We suggest, that polarization-sensitive photoreceptors contributed to the UV-sensitivity peak of *E. virgo* compound eyes. Our setup allowed only extracellular recordings, but it would be interesting to test the polarization and spectral sensitivity of single photoreceptors of *E. virgo* or other twilight-swarming mayflies with intracellular recordings. This could also reveal the presence of blue receptors. The significant shift towards the shorter wavelengths of the fitted green pigment template for adults might be related to the presence of blue receptors that do not necessarily undergo sensitivity decrease like the green ones.

Anyone who has once seen the mass swarming of a twilight-swarming mayfly, such as *E. virgo*, knows how fascinating the appearance, presence and vanishing of the mayflies over the river within the relatively short time frame of the twilight is (electronic supplementary material, movies S3 and S4). The underlying mechanism behind the strict timing of the swarming of *E. virgo*, and other twilight-swarming mayflies is still a mystery but temperature and light intensity might play a role in triggering the swarming [1]. An interesting behavioural experiment would be to test the effect of the spectrum of overhead illumination on the timing of emergence.

Ethics

Permission for collecting *E. virgo* individuals was obtained from the Government Office for Pest County of Hungary (document no. PE-06/KTF/04563-6/2020 and PE-06/KTF/04563-7/2020)

Data accessibility

Source code, receptor response amplitudes, data of spectral and transmittance measurements and swarming intensity data are available from the Dryad Digital Repository [40]. https://doi.org/10.5061/dryad.zpc866tb0.

Authors' contributions:

Á.E.: conceptualization, funding acquisition, investigation, methodology, software, supervision, visualization, writing–original draft and writing–review and editing; Á.M.: investigation and visualization; G.K.: conceptualization, funding acquisition, supervision, visualization, writing–original draft and writing–review and editing.

All authors gave final approval for publication and agreed to be held accountable for the work performed therein.

Conflict of interest declaration

The authors declare no competing interests.

Funding

Project no. 131738 has been implemented with the support provided from the National Research, Development and Innovation Fund of Hungary, financed under the PD_19 funding scheme. The project was supported by the ÚNKP-21-3 New National Excellence Program of the Ministry for Innovation and Technology from the source of the National Research, Development and Innovation Fund. We are grateful to Jan Gershoj (Gershoj Energia Kft, Hungary) for his kind support.

Acknowledgements

We are grateful to the Government Office for Pest County (Hungary) for giving us permission for collecting individuals of the protected *E. virgo* mayflies. We are also grateful to the Időkép Weather Service Ltd. (https://www.idokep.hu) for providing the webcam images. We thank Ferenc Kriska for his help in recording the supplementary videos.

Data availability

The data that support the findings of this study are available from the corresponding author upon request.

References

1. Sartori M, Brittain JE. 2015 Order Ephemeroptera. In *Thorp and Covich's Freshwater Invertebrates: Ecology and General Biology* (eds JH Thorp, DC Rogers), pp. 873–891. London, UK: Academic Press.
2. Kureck A. 1992 Das Massenschwärmen der Eintagsfliegen am Rhein. Zur Rückkehr von *Ephoron virgo* (Olivier 1791). *Nat. Landsch.* **67**, 407–409.
3. Tobias W. 1996 Sommernächtliches 'Schneetreiben'am Main: Zum Phänomen des Massenfluges von Eintagsfliegen. *Nat. Mus.* **126**, 37–57.
4. Kazanci N, Türkmen G. 2015 The swarm of *Ephoron virgo* (Olivier, 1791) (Ephemeroptera: Polymitarcyidae) in Kura River (Turkey). *Rev. Hydrobiol.* **8**, 63–65.

5. Száz D, Horváth G, Barta A, Robertson BA, Farkas A, Egri Á, Tarjányi N, Rácz G, Kriska G. 2015 Lamp-lit bridges as dual light-traps for the night-swarming Mayfly, *Ephoron virgo*: Interaction of polarized and unpolarized light pollution. *PLOS ONE* **10**, e0121194. (doi:10.1371/journal.pone.0121194)
6. Kriska G. 2013 *Freshwater Invertebrates in Central Europe*. Vienna: Springer Vienna. (doi:10.1007/978-3-7091-1547-3)
7. Cid N, Ibáñez C, Prat N. 2008 Life history and production of the burrowing mayfly *Ephoron virgo* (Olivier, 1791) (Ephemeroptera: Polymitarcyidae) in the lower Ebro river: A comparison after 18 years. *Aquat. Insects* **30**, 163–178. (doi:10.1080/01650420802010356)
8. Marković V, Kračun-Kolarević M, Kolarević S, Tubić B, Ilić M, Nikolić V, Paunović M. 2017 A first record of *Ephoron virgo* (Olivier, 1791) (Ephemeroptera: Polymitarcyidae) from the Sava River, with notes on its ecological preferences and rarity of findings in the region. *Ecol. Montenegrina* **13**, 80–85.
9. Kureck A, Fontes RJ. 1996 The life cycle and emergence of *Ephoron virgo*, a large potamal mayfly that has returned to the river Rhine. *Arch. Hydrobiol. Suppl.* **113**, 319–323. (doi:10.1127/lr/10/1996/319)
10. Lancaster J. 2013 *Aquatic entomology*. 1st ed. Oxford: Oxford University Press.
11. Russev BK. 1973 Kompensationsflug bei der Ordnung Ephemeroptera. In *Proceedings of the 1st International Conference on Ephemeroptera*, pp. 132–142. Leiden: E.J. Brill.
12. Egri Á, Száz D, Farkas A, Pereszlényi Á, Horváth G, Kriska G. 2017 Method to improve the survival of night-swarming mayflies near bridges in areas of distracting light pollution. *R. Soc. Open Sci.* **4**, 171166. (doi:10.1098/rsos.171166)
13. Mészáros Á, Kriska G, Egri Á. 2021 Spectral optimization of beacon lights for the protection of night-swarming mayflies. *Insect Conserv. Divers.* **14**, 225–234. (doi:10.1111/icad.12446)
14. Durmus D, Wang J, Good S, Basom B. 2021 The effect of electric bridge lighting at night on mayfly activity. *Energies* **14**, 2934. (doi:10.3390/en14102934)
15. Cronin TW, Johnsen S, Marshall NJ, Warrant EJ. 2014 *Visual Ecology*. Princeton: Princeton University Press.
16. Gupta S, Gupta A, Meyer-Rochow VB. 2000 Post-embryonic development of the lateral eye of *Cloeon* sp. (Ephemeroptera: Baetidae) as revealed by scanning electron microscopy. *Entomol. Fennica* **11**, 89–96. (doi:10.33338/ef.84049)
17. Kecskeméti S, Geösel A, Fail J, Egri Á. 2021 In search of the spectral composition of an effective light trap for the mushroom pest *Lycoriella ingenua* (Diptera: Sciaridae). *Sci. Rep.* **11**, 12770. (doi:10.1038/s41598-021-92230-y)
18. Egri Á, Kriska G. 2019 How does the water springtail optically locate suitable habitats? Spectral sensitivity of phototaxis and polarotaxis in *Podura aquatica*. *J. Exp. Biol.* **222**, jeb199760. (doi:10.1242/jeb.199760)
19. Allan SA, Stoffolano Jr. JG, Bennett RR. 1991 Spectral sensitivity of the horse fly *Tabanus nigrovittatus* (Diptera: Tabanidae). *Can. J. Zool.* **69**, 369–374. (doi:10.1139/z91-057)
20. Govardovskii VI, Fyhrquist N, Reuter T, Kuzmin DG, Donner K. 2000 In search of the visual pigment template. *Vis. Neurosci.* **17**, 509–528. (doi:10.1017/S0952523800174036)
21. Nelder JA, Mead R. 1965 A simplex method for function minimization. *Comput. J.* **7**, 308–313. (doi:10.1093/comjnl/7.4.308)
22. Spitschan M, Aguirre GK, Brainard DH, Sweeney AM. 2016 Variation of outdoor illumination as a function of solar elevation and light pollution. *Sci. Rep.* **6**, 26756. (doi:10.1038/srep26756)
23. Johnsen S. 2012 *The Optics of Life*. Princeton University Press. (doi:10.2307/j.ctt7s4q4)
24. Meyer-Rochow VB. 1982 Electrophysiological studies on the insect compound eye. *N. Z. Entomol.* **7**, 296–304. (doi:10.1080/00779962.1982.9722403)
25. Horridge GA, McLean M. 1978 The dorsal eye of the mayfly Atalophlebia (Ephemeroptera). *Proc. R. Soc. Lond. B* **200**, 137–150. (doi:10.1098/rspb.1978.0011)

26. Heise BA. 1992 Sensitivity of mayfly nymphs to red light: Implications for behavioural ecology. *Freshw. Biol.* **28**, 331–336. (doi:10.1111/j.1365-2427.1992.tb00591.x)
27. Hughes DA. 1965 Preliminary investigations of the light responses of Ephemeroptera nymphs. *S. Afr. J. Sci.* **61**, 397–403.
28. Elliott JM. 2009 The daily activity patterns of mayfly nymphs (Ephemeroptera). *J. Zool.* **155**, 201–221. (doi:10.1111/j.1469-7998.1968.tb03039.x)
29. Kühne JL, van Grunsven RHA, Jechow A, Hölker F. 2021 Impact of different wavelengths of artificial light at night on phototaxis in aquatic insects. *Integr. Comp. Biol.*, icab149. (doi:10.1093/icb/icab149)
30. Eguchi E, Watanabe K, Hariyama T, Yamamoto K. 1982 A comparison of electrophysiologically determined spectral responses in 35 species of Lepidoptera. *J. Insect Physiol.* **28**, 675–682. (doi:10.1016/0022-1910(82)90145-7)
31. Meyer-Rochow VB, Horridge GA. 1975 The eye of *Anoplognathus* (Coleoptera, Scarabaeidae). *Proc. R. Soc. Lond. B.* **188**, 1–30. (doi:10.1098/rspb.1975.0001)
32. Lunau K, Knüttel H. 1995 Vision through colored eyes. *Naturwissenschaften* **82**, 432–434. (doi:10.1007/BF01133678)
33. Chou A, Lin C, Cronin TW. 2020 Visual metamorphoses in insects and malacostracans: Transitions between an aquatic and terrestrial life. *Arthropod Struct. Dev.* **59**, 100974. (doi:10.1016/j.asd.2020.100974)
34. Almudi I *et al.* 2020 Genomic adaptations to aquatic and aerial life in mayflies and the origin of insect wings. *Nat. Commun.* **11**, 2631. (doi:10.1038/s41467-020-16284-8)
35. Oba Y, Kainuma T. 2009 Diel changes in the expression of long wavelength-sensitive and ultraviolet-sensitive opsin genes in the Japanese firefly, *Luciola cruciata*. *Gene* **436**, 66–70. (doi:10.1016/j.gene.2009.02.001)
36. Hariyama T, Meyer-Rochow VB, Eguchi E. 1986 Diurnal changes in structure and function of the compound eye of *Ligia exotica* (Crustacea, Isopoda). *J. Exp. Biol.* **123**, 1–26. (doi:10.1242/jeb.123.1.1)
37. Farkas A, Száz D, Egri Á, Barta A, Mészáros Á, Hegedüs R, Horváth G, Kriska G. 2016 Mayflies are least attracted to vertical polarization: A polarotactic reaction helping to avoid unsuitable habitats. *Physiol. Behav.* **163**, 219–227. (doi:10.1016/j.physbeh.2016.05.009)
38. Schwind R. 1995 Spectral regions in which aquatic insects see reflected polarized light. *J. Comp. Physiol. A* **177**, 439–448. (doi:10.1007/BF00187480)
39. Bernath B, Gál J, Horváth G. 2004 Why is it worth flying at dusk for aquatic insects? Polarotactic water detection is easiest at low solar elevations. *J. Exp. Biol.* **207**, 755–765. (doi:10.1242/jeb.00810)
40. Egri Á, Mészáros Á, Kriska G. 2022 Spectral sensitivity transition in the compound eyes of a twilight-swarming mayfly and its visual ecological implications. *Dryad Digital Repository* (doi:10.5061/dryad.zpc866tb0)

Supplementary material for *Spectral sensitivity transition in the compound eyes of a twilight-swarming mayfly and its visual ecological implications*

This document contains Supplementary Figures S1-3 and captions for Supplementary Movies S1-5.

Figure S1: Evaluation of webcam images for determining the swarming period of *E. virgo* within the day, as a function of solar elevation θ. (A) Webcam image from 5 September 2019 during the day at 12:26 (UTC + 2h). (B) Webcam image from the same day at 20:33 (UTC + 2h). Yellow rectangle shows the cropped region of the image that was used in further evaluation. (C) Sub-image shown by yellow rectangle in B (size = 90 × 72 pixels). (D) Median image of the 267 cropped sub-images taken after sunset on 5 September 2019. This image is the mayfly-free static background, that was calculated by obtaining the median pixel intensity at each pixel position across all sub-images. (E) Greyscale version of the difference of D and C where the bright pixels on a black background indicate the presence of swarming mayflies. Overall brightness values (mean pixel intensity) of these kind of images were plotted against solar elevation θ in Fig. S3.

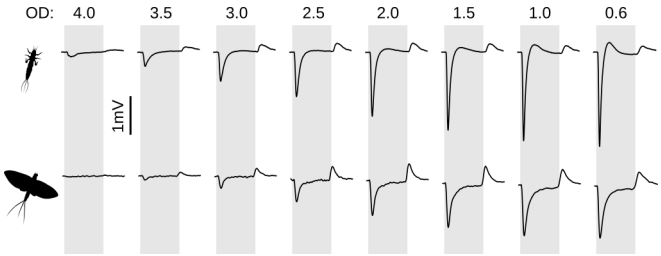

Figure S2: Typical measured receptor responses of a female *E. virgo* larva (upper row) and a female adult (lower row) eye preparation elicited by 516 nm light stimuli. Grey regions represent the 500-ms-long stimuli. Numbers at the top indicate the photon flux of stimuli in optical density units, where OD = $-\log_{10}(I/I_0)$ and $I_0 = 7.6 \cdot 10^{14}$ photons/cm^2/s.

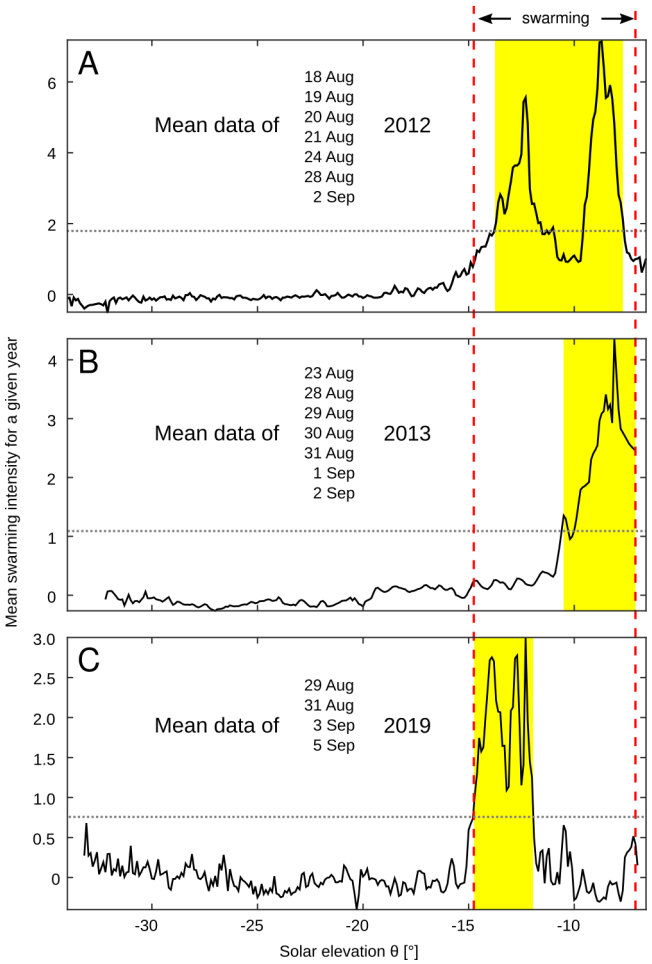

Figure S3: Calculated mean overall brightness of processed webcam sub-images (Fig. S1E) for evaluated days of 2012 (A), 2013 (B) and 2019 (C). Solar elevation ranges shown by yellow rectangles correspond to full widths at 25% maximum of the data (horizontal dotted lines show 25% of maximum). The union of these yearly ranges, indicated by red vertical dashed lines, was considered as the typical solar elevation range for the swarming of *E. virgo* mayflies: -14.7° < θ < -7.1°.

Movie S1: Larvae of the virgin mayfly (E. virgo) on river-bottom sediments. The digging behaviour is typical for a burrowing mayfly like E. virgo, that live inside the uppermost layer of the bottom. This video was recorded by György Kriska.

Movie S2: Final moult of a newly emerged male E. virgo subimago. Females do not need this additional moult as they become immediately mature adults after emergence. This video was recorded by Ferenc Kriska.

Movie S3: Mass swarming of E. virgo at the Zoltán Tildy bridge in Tahitótfalu (Northern Hungary) in 2012. Because the mayflies swarm after sunset, the bridge lighting attracted enormous amounts of mayflies. In the second section of the movie, individuals dying on the asphalt with their yellow egg-batches can be seen. This video was recorded by György Kriska.

Movie S4: Mass swarming of E. virgo at the Zoltán Tildy bridge in Tahitótfalu (Northern Hungary) in 2019. In the first part, a time lapse video of the mayfly-protecting beacon lights at the piers of the Zoltán Tildy bridge [13] is shown. The second part shows swarming E. virgo individuals. The last part shows the previously mentioned beacons in action, during mass swarming (with a boat on the scene). This video was created by Ferenc Kriska.

Movie S5: Egg laying E. virgo females at the river surface. This slow-motion video shows oviposition on the water surface and eggs reaching the bottom. This video was recorded by Ferenc Kriska.